

# Magnetofluidization of Fine Magnetite Particles

Cite as: AIP Conference Proceedings **1145**, 119 (2009); <https://doi.org/10.1063/1.3179843>  
Published Online: 01 July 2009

M. A. S. Quintanilla, M. J. Espin, J. M. Valverde, and A. Castellanos



View Online



Export Citation

## ARTICLES YOU MAY BE INTERESTED IN

[Analysis of Tribo-Electric Charging of Spherical Beads Using Distinct Element Method](#)  
AIP Conference Proceedings **1145**, 127 (2009); <https://doi.org/10.1063/1.3179845>

Lock-in Amplifiers  
up to 600 MHz



# Magnetofluidization of Fine Magnetite Particles

M.A.S. Quintanilla\*, M. J. Espin<sup>†</sup>, J. M. Valverde\* and A. Castellanos\*

\*Faculty of Physics. University of Seville. Avenida Reina Mercedes s/n, 41012 Seville, Spain.

<sup>†</sup>Department of Applied Physics II. University of Seville. Avenida Reina Mercedes s/n, 41012 Seville, Spain.

**Abstract.** In this study we investigate the behaviour of a fluidized bed of fine magnetite particles as affected by a cross-flow uniform magnetic field. Due to the small particle size (35 microns), the fluidized system displays a typical Geldart A fluidization behaviour in the absence of an external field, i.e. natural van der Waals forces are able to stabilize fluidization in a short interval of gas velocities above the minimum fluidization velocity. The effect of the external field is to delay bed stability to higher gas velocities. Mechanical measurements on the magnetofluidized bed have been carried out using the Seville Powder Tester, which allows us for an accurate control of gas flow, and measurement of gas pressure drop across the bed and bed height. The tensile strength of the magnetically stabilized bed has been tested as a function of the gas velocity.

**Keywords:** Fluidized beds, magnetofluidization, fine cohesive powders

**PACS:** 47.55.Lm, 61.43.Gt, 47.65.-d

## INTRODUCTION

Bubbling fluidization is the common behavior found in fluidized beds of coarse granules (typically of size  $d_p > 100 \mu\text{m}$ ) as soon as the gas velocity surpasses the minimum fluidization velocity  $v_{mf}$ . This type of behavior is the so-called Geldart B behavior according to the Geldart's diagram [1], which was originally derived from empirical observations on beds fluidized by air at ambient conditions. For intermediate size particles ( $d_p$  typically between  $20 \mu\text{m}$  and  $50 \mu\text{m}$ ), the van der Waals attractive forces between the particles become comparable to particle weight and are capable of suppressing bubbles in an interval of gas velocities between  $v_{mf}$  and  $v_g = v_b > v_{mf}$ , where  $v_b$  is the gas velocity at bubbling instability (Geldart A behavior [1]). In the stable state, interparticle contacts are permanently held by the attractive forces, the bed is jammed and takes the appearance of a weak solid. Fluidlike behavior is accompanied by the instability to bubbling when the gas velocity just equals  $v_b$ . Artificial enhancement of interparticle forces has been investigated as a tool to suppress the growth of gas bubbles in the fluidization of Geldart's B coarse granular materials. For example, bubbling beds of ferromagnetic particles can be stabilized by application of a magnetic field [2]. This results in the formation of strings of magnetized particles that eventually become jammed. Most studies on magnetic field stabilization deal with the behavior of relatively large grains (Geldart B granular materials), showing just bubbling fluidization in the absence of field. In our work we investigate the magnetofluidization behavior of naturally cohesive fine magnetite powder, which belongs to the class of Geldart A powders, i.e. the fluidized state of this powder can be naturally stabilized by van der Waals forces alone.

## EXPERIMENTAL SETUP

The powder sample is held in a vertically oriented cylindrical vessel (2.54cm internal diameter in the experiments reported in this paper) and rests on a porous plate that acts as gas distributor ( $5\mu\text{m}$  pore size). By means of a series of computer controlled valves and a mass flow controller, a controlled flow of filtered and dried air is pumped through the powder bed while the gas pressure drop across it is read from a differential pressure transducer. The height of the bed, which gives an average value of the particle volume fraction  $\phi$ , is measured by means of an ultrasonic sensor placed on top of the vessel. This magnetic powder is tested as affected by a cross-flow uniform magnetic field externally imposed. The magnetic field strength is varied by adjusting the electrical current through a pair of square Helmholtz coils ( $50 \times 50 \text{ cm}$ ) with 500 turns each of 2 mm dia. copper wire around each coil. The magnetic field strength is measured by means of a transverse probe with an accuracy of 0.1 mT. The material used in the experiments is magnetite powder. Average particle size and particle density are  $35 \mu\text{m}$  and  $5060 \text{ kg/m}^3$ , respectively. This powder was not permanently magnetized. In order to induce permanent magnetism on artificial magnetite comparable in strength with permanently magnetized natural magnetite, fields strengths of 100 kA/m or higher are necessary [3]. In our study the applied field strength  $H_0$  is typically below 5 kA/m. For these small fields applied, particle magnetization  $\mathbf{M}_p$  would be related to the externally imposed field  $\mathbf{H}_0$  by means of the linear relationship  $\mathbf{M}_p = \chi_p \mathbf{H}_0$ , where  $\chi_p$  is the initial particle susceptibility. Mills reports values between 2.3 and 12.6 for the initial susceptibility of Magnet Cove magnetite [3]. We have obtained  $\chi_p$  by measuring in our experi-

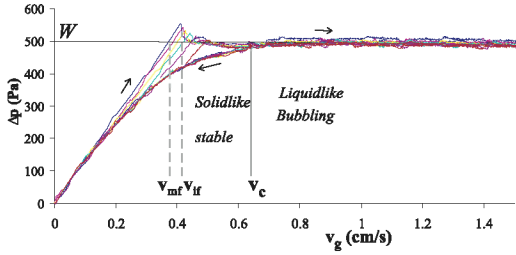


**FIGURE 1.** (color online) Gas pressure drop across the magnetite powder bed as a function of superficial gas velocity during the fluidization-defluidization cycles in the absence of externally imposed magnetic field. The transition to solidlike stable fluidization at  $v_c$  (jamming transition) is delineated. The minimum fluidization velocity  $v_{mf}$  and incipient fluidization velocity  $v_{if}$  for the bed settled under its own weight are indicated.

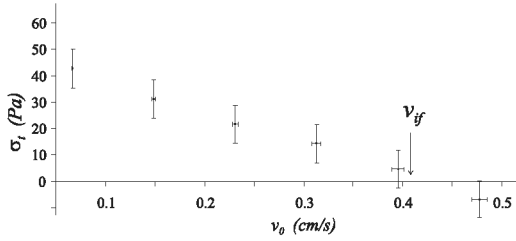


**FIGURE 2.** Tensile strength of the bed as a function of the gas velocity during defluidization. The gas velocity at incipient fluidization  $v_{if}$  of the bed settled under its own weight ( $v_0 = 0$  cm/s) is indicated.

mental setup the strength of the field at a fixed point with and without the powder bed present. It has been seen that the bulk magnetization increases linearly as the strength of the external field  $H_0$  is increased, and can be well fitted by the equation  $M = 1.81H_0$  A/m. From the Bruggeman relation [4]  $(1 - \phi)(\chi_0 - \chi)/(3 + \chi_0 + 2\chi) + \phi(\chi_p - \chi)/(3 + \chi_p + 2\chi) = 0$ , where in our case  $\chi_0 = 0$  is the gas susceptibility,  $\chi = 1.81$  is the bulk susceptibility, and  $\phi = 0.48$  is the particle volume fraction, it is obtained  $\chi_p = 5.33$ , which is similar to the values reported in the literature for magnetite solids that were not permanently magnetized [3].

## EXPERIMENTAL RESULTS AND DISCUSSION

Figure 1 shows data of the gas pressure drop across the magnetite powder bed  $\Delta p$  measured as a function of the superficial gas velocity  $v_g$  and in the absence of externally applied magnetic field. In these tests, the powder is first driven to the bubbling regime by imposing a gas velocity  $v_g = 2$  cm/s. Once the bubbling bed has reached

a stationary state, in which it has lost memory of its previous history [5], the gas flow is suddenly turned off and the bed is allowed to settle. The settled powder layer is then subjected to a slowly increasing gas flow. At first the bed structure is unperturbed and  $\Delta p$  increases linearly as  $v_g$  is increased (see Fig. 1). At the point of minimum fluidization velocity ( $v_g = v_{mf} \simeq 0.39$  cm/s, see Fig. 1)  $\Delta p$  balances  $W$ . At this point a powder with zero cohesion will become fluidized, yet the pressure drop across our naturally cohesive powder continues to increase above the minimum fluidization velocity. Above this point the gas flow puts the bed under tension, and as the tension builds up there comes a point at which the powder breaks in tension and the pressure drop falls down to around the weight per unit area (see Fig. 1). This is the point of incipient fluidization ( $v_g = v_{if} \simeq 0.41$  cm/s). The condition for tensile yield is met first at the bottom of the bed, where the fracture of the bed is observed to start as it is theoretically expected [5]. Provided that wall effects are negligible, the tensile strength  $\sigma_t$  of the settled powder is given by the difference between the pressure drop across the bed just before the breaking and the weight per unit area  $\sigma_t = (\Delta p)_{max} - W \simeq 43$  Pa. Further increase of the gas velocity gives rise to a state of heterogeneous fluidization, whose main characteristic is the propagation of the fracture in the upward direction while  $\Delta p$  fluctuates around the powder weight per unit area  $W$ . Large visible bubbles are seen to be developed at  $v_g = v_b \simeq 0.8$  cm/s, coinciding with a maximum of bed expansion. If the gas flow is now decreased from the bubbling regime, the typical hysteretic behavior of Geldart's A powders becomes apparent at a gas velocity  $v_g = v_c \simeq 0.65$  cm/s, in which the powder bed is jammed, and  $\Delta p < W$  since part of the weight is sustained by the enduring interparticle contacts. If the gas flow during the defluidization part of the cycle is increased again from  $v_0$ , it is seen that  $\Delta p$  increases linearly as  $v_g$  is increased (see Fig. 1). Note that the slope of this straight line is smaller than the slope for the bed settled under its own weight ( $v_0 = 0$  cm/s), indicating a smaller particle volume fraction of the stably fluidized bed at a gas velocity  $v_0$  as should correspond to an expanded state. The new pressure overshoot enables us to measure the tensile strength of the bed  $\sigma_t$  in the under-consolidated state. In figure 2 the tensile strength of the fluidized bed as measured through this process are shown as a function of  $v_0$ . As expected,  $\sigma_t$  decrease as  $v_0$  is increased. Within the accuracy of our pressure drop measurements, the tensile strength  $\sigma_t$  becomes insignificant when the gas velocity  $v_0$  is larger than the incipient fluidization velocity  $v_{if} \simeq 0.41$  cm/s. The practically zero value of the tensile strength measured for gas velocities above incipient fluidization ( $v_0 > 0.41$  cm/s) may be rationalized from a simple estimation of the value of the interparticle attractive force  $f$ . In the absence of particle magnetization the dominant interparticle force is the van

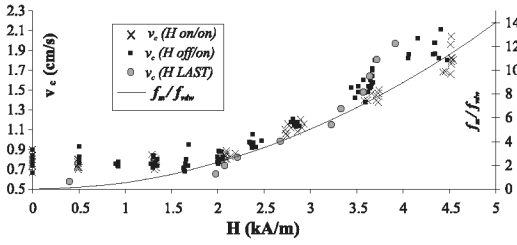


**FIGURE 3.** Left axis: Gas velocity at the transition to the solidlike stabilized state  $v_c$  as a function of the magnetic field strength according to both operation modes used in the fluidization-defluidization cycles. Data from magnetization LAST experiments are shown for comparison. Right axis: ratio of the attractive interparticle magnetic force to the attractive interparticle van der Waals force.

der Waals attractive force, which can be approximated by [5]  $f_{vdW} \simeq Ad_a/24z_0^2$ , where  $A$  is the Hamaker constant,  $z_0 \simeq 3 - 4 \text{ \AA}$  is the distance of closest approach between two molecules and  $d_a$  is the typical size of the surface asperities  $d_a$ . A typical value reported for the size of surface asperities of fine powder particles is  $d_a \simeq 0.2 \mu\text{m}$  [5], while the reported values of  $A$  for most materials is around  $10^{-19} \text{ J}$  [5]. Thus we can estimate an attractive force  $f_{vdW} \simeq 10 \text{ nN}$  between our experimental particles. The bulk tensile strength of the powder that arises from the existence of an interparticle attractive force  $f$  can be estimated by means of the Rumpf averaging equation [5] as  $\sigma_t \sim f\zeta\phi/\pi d_p^2$ , where  $\zeta$  is the coordination number (average number of contacts per particle) that can be related to the particle volume fraction  $\phi$  by the equation  $\zeta \simeq (\pi/2)(1 - \phi)^{-3/2}$ . Using as typical values  $f = f_{vdW} = 10 \text{ nN}$ ,  $d_p = 35 \mu\text{m}$ , and  $\phi = 0.4$ , it is estimated  $\sigma_t \simeq 4 \text{ Pa}$ , which is about our experimental indeterminacy. As the gas velocity is decreased below the incipient fluidization velocity ( $v_0 < 0.41 \text{ cm/s}$ ), the powder is consolidated under its own weight force and plastic deformation of interparticle contacts increases the interparticle attractive force [5], thus increasing the tensile strength.

The measuring process described above has been performed for different values of the strength of an applied cross-flow magnetic field. This is accomplished by applying the field when the bed is in the initial bubbling regime, preceding any measurement, and it is held constant during the defluidization part of the cycle. In this way, the gas velocity at the transition to the solidlike stabilized state  $v_c$  can be identified by looking at the initiation of hysteresis in the fluidization-defluidization cycles ( $\Delta p < W$ ). Additionally, we have investigated whether the mechanical strength of the stably fluidized bed can be affected by application of an external field. The procedure followed to measure the tensile strength is the same as done in the absence of the field. The application of the

field has been performed in two different modes. In one mode (termed as *H on*) the bed is initialized by applying a high gas velocity ( $v_g = 2 \text{ cm/s}$ ) that drives it to bubbling in the presence of field. Then the bed is allowed to settle at a remanent gas velocity  $v_0$  while the magnetic field is kept constant. In this state the bed is stabilized both by natural and magnetic interparticle cohesive forces. In the other mode (termed as *H off/on*), and once the fluidized bed reaches a magnetically stabilized state at a gas velocity  $v_0 < v_c$ , the magnetic field is turned off and the bed is driven to bubbling in the absence of field. The bed is then allowed to settle at the gas velocity  $v_0$ . In this state the bed remains stabilized just by the natural interparticle cohesive forces. After settling, the field is turned on again and the tensile strength is measured.

The transition velocity  $v_c$  from the bubbling regime to the stable solidlike state (jamming transition) is plotted in Fig. 3 as a function of the magnetic field strength (left axis). A remarkable result is that, in the presence of magnetic field, the jamming transition occurs at higher gas velocities as compared with the transition velocity in the absence of external field. The field effect becomes noticeable for strengths roughly above  $2 \text{ kA/m}$ . For  $H > 2 \text{ kA/m}$ ,  $v_c$  increases steadily as the magnetic field strength is increased.

In the range of field strengths applied, the dipolar approximation can be used for an estimation of order of magnitude of the contact force [7]. The attractive force between two aligned dipoles of moment  $m_p$  separated by a distance  $d_p$  is given by  $f_m = 3\mu_0 m_p^2 / 2\pi d_p^4$ , where  $\mu_0$  is the permeability of free space ( $4\pi \times 10^{-7} \text{ H/m}$ ). According to our rheological measurements, in the presence of an external field, the magnetite particles would be magnetized with a dipolar moment  $m_p = \chi_p H_0 (1/6)\pi d_p^3$ . In Fig. 3 we have plotted the ratio  $f_m/f_{vdW}$  (right axis) as a function of the magnetic field strength. It is observed that the increase of  $v_c$  begins at the point in which the magnetic force becomes around twice the van der Waals force. For smaller fields, the magnetic and van der Waals forces are comparable or smaller and there is not an observable effect of the magnetic field on the jamming transition. As the magnetic field is increased above  $H \simeq 2 \text{ kA/m}$ ,  $v_c$  increases proportionally to the increase of  $f_m/f_{vdW}$  ( $\Delta v_g \propto f_m/f_{vdW}$ ). In Fig. 4 the measured values of  $\phi$  at  $v_g = v_c$  are plotted as a function of the magnetic field strength. In agreement with the previous analysis on  $v_c$ , it is also seen that the effect of the field becomes relevant for field strengths above  $2 \text{ kA/m}$ . It is observed that the values of  $\phi$  measured at  $v_g = v_c$  using the *H on* mode are generally larger than the corresponding ones measured using the *H off/on* operation mode. In the *H on* mode, the field affects the packing of the jammed bed possibly by means of the formation of structures of aligned particle dipoles during liquidlike fluidization due

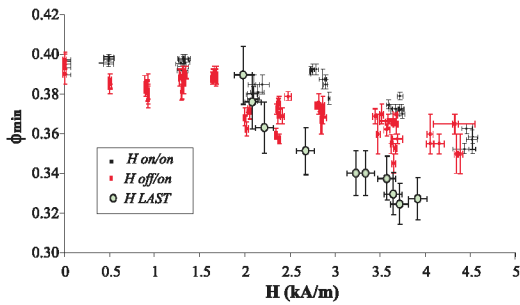


**FIGURE 4.** (color online) Particle volume fraction  $\phi$  of the fluidized bed at the jamming transition vs. the strength of the magnetic field according to the two different operation modes (symbols in black:  $H$  on; symbols in red:  $H$  off/on. Data from Magnetization LAST experiments are also shown.

to particle magnetization and reorientation in the presence of the field. On the other hand, in the  $H$  on mode, bed restructuring is not allowed since the field is applied after the bed is jammed and the particles have lost their freedom to rearrange. In this state it is unlikely that the field changes the packing structure of the jammed bed.

In magnetization LAST experiments, the fluidized bed is subjected to a fixed gas velocity above the bubbling velocity in the absence of magnetic field. Then, the magnetic field strength is slowly increased from zero to look for the magnetic field strength at the jamming transition. As the field strength is increased it is seen that at a certain field strength bubbles are suppressed. If the field strength is slightly further increased above this critical value, the bed is jammed. It is noticed also that jamming causes an additional small expansion that is accompanied by the visualization of particle chains at the bed free surface. In Fig. 3 experimental data on the jamming field as a function of the gas velocity are shown. Within the experimental scatter, the data fits to the same trend that follows the data obtained by means of the previous procedure, in which the gas velocity was decreased for a fixed field strength. Note however that the values of the particle volume fraction (Fig. 4) at magnetic stabilization are clearly smaller in the magnetization LAST experiments. This effect can be attributed to the quasistatic increase of the field strength at fixed gas velocity that allows for a highly expanded structure at jamming.

Tensile strength data as a function of the strength of the magnetic field are plotted in Fig. 5 for different values of the remanent gas velocity  $v_0$  at jamming. It is observed that application of the field to the naturally stabilized bed ( $H$  off/on mode) does not play an important role for field strengths  $H < 2$  kA/m. For fields of higher strengths ( $H > 2$  kA/m), the tensile strength increases slightly as the field strength is increased. On the other hand, application of the field during fluidization and settling ( $H$  on mode) does produce a noticeable increase of the tensile

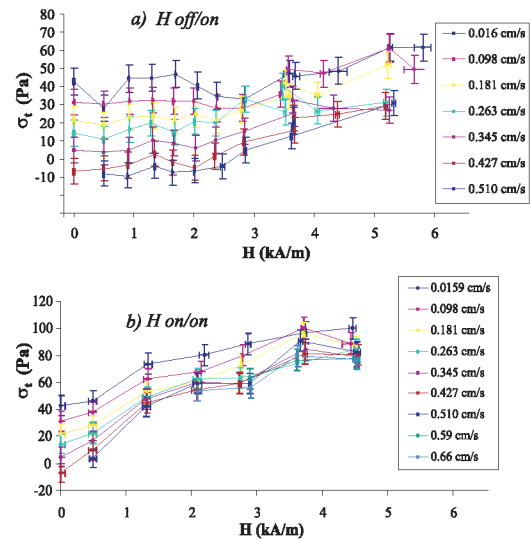


**FIGURE 5.** (color online) Tensile strength of the magnetically jammed bed as a function of the strength of the magnetic field for different values of the gas velocity  $v_0$  (shown in the inset) and according to both operation modes. The lines are a guide to the eye.

strength of the bed as it was previously noted. A reasonable explanation is that in the fluidized state, particles are free to rotate and, being magnetized by the external field, are prone to form strong particle chains that strengthen the jammed bed when the gas velocity is decreased ( $H$  on operation mode). In contrast, if the magnetic field is turned off in the fluidized state and turned on again once the bed is jammed ( $H$  off/on operation mode), the magnetized particles are constrained and their restructuring is not allowed.

## ACKNOWLEDGMENTS

We acknowledge Spanish Government Agency Ministerio de Ciencia y Tecnología (contract FIS2006-03645) and Junta de Andalucía (contract FQM 421).

## REFERENCES

1. D. Geldart, Powder Technol. 7 (1973) 285–293.
2. R. E. Rosensweig, Ferrohydrodynamics (Dover publications, New York, 1997).
3. A. A. Mills, Annals of Science, 61 (2004) 273–319.
4. K. Karkkainen, A. Sihvola, K. Nikoskinen, IEEE Trans. Geosci. Remote Sensing., 39 (2001) 1013–1018.
5. A. Castellanos, Adv. Phys. 54 (2005) 263–376.
6. T. B. Jones, G. L. Whittaker, T. J. Sulenski, Powder Technol. 49 (1987) 149–164.
7. C. Tan, T. B. Jones, J. Appl. Phys. 73 (1993) 3593–3598.